Photobleaching Recovery and Anisotropy Decay of Green Fluorescent Protein GFP-S65T in Solution and Cells: Cytoplasmic Viscosity Probed by Green Fluorescent Protein Translational and Rotational Diffusion

R. Swaminathan, Cathy P. Hoang, and A. S. Verkman
Departments of Medicine and Physiology, Cardiovascular Research Institute, University of California, San Francisco, California 94143 USA

ABSTRACT The green fluorescent protein (GFP) was used as a noninvasive probe to quantify the rheological properties of cell cytoplasm. GFP mutant S65T was purified from recombinant bacteria for solution studies, and expressed in CHO cell cytoplasm. GFP-S65T was brightly fluorescent in solution (λ_{ex} 492 nm, λ_{em} 509 nm) with a lifetime of 2.9 ns and a rotational correlation time (t_c) of 20 ns. Recovery of GFP fluorescence after photobleaching was complete with a half-time ($t_{1/2}$) in aqueous saline of 30 ± 2 ms (5-μm diameter spot), giving a diffusion coefficient of 8.7×10^{-7} cm^2/s. The $t_{1/2}$ was proportional to solution viscosity and was dependent on spot diameter. In contrast to fluorescein, GFP photobleaching efficiency was not affected by solution O_2 content, triplet state quenchers, singlet oxygen scavengers, and general radical quenchers. In solutions of higher viscosity, an additional, rapid GFP recovery process was detected and ascribed to reversible photobleaching. The $t_{1/2}$ for reversible photobleaching was 1.5–5.5 ms (relative viscosity 5–250), was independent of spot diameter, and was unaffected by O_2 or quenchers. In cell cytoplasm, time-resolved microfluorimetry indicated a GFP lifetime of 2.6 ns and a t_c of 36 ± 3 ns, giving a relative viscosity (cytoplasm versus water) of 1.5. Photobleaching recovery of GFP in cytoplasm was 82 ± 2% complete with a $t_{1/2}$ of 83 ± 6 ms, giving a relative viscosity of 3.2. GFP translational diffusion increased 4.7-fold as cells swelled from a relative volume of 0.5 to 2. Taken together with measurements of GFP translation and rotation in aqueous dextran solutions, the data in cytoplasm support the view that the primary barrier to GFP diffusion is collisional interactions between GFP and macromolecular solutes.

INTRODUCTION

The green fluorescent protein (GFP) from the jellyfish *Aequorea victoria* is now used widely as a noninvasive fluorescent marker for gene expression and protein localization (Gerdes and Kaether, 1996; Chalfie et al., 1994; Cubitt et al., 1995). GFP has been expressed alone or in fusion with various proteins in bacteria, plants, yeast, mammalian cells, and whole organisms. In mammalian cells in culture, GFP fusion proteins have been targeted to specific organelles and subcellular sites using organelle-specific targeting sequences, or by fusion with endogenous protein markers (Rizzuto et al, 1995, 1996; Giorgi et al., 1996; Cole et al., 1996). Numerous applications in cell biology are being developed in the areas of vesicular transport, exocytosis, protein processing, and membrane dynamics.

A potentially useful application for GFP is as a probe to study the viscous properties of intracellular aqueous compartments using photobleaching recovery and time-resolved fluorescence methods. Studies of macromolecule translational mobility in cytoplasm have required invasive microinjection procedures to introduce fluorescent probes (Luby-Phelps, 1994). GFP offers a noninvasive approach to label many intracellular compartments with high specificity. For example, studies of macromolecule diffusion are of particular interest in mitochondria, where the "metabolic channeling" hypothesis proposes that the mitochondrial matrix is too crowded for aqueous-phase diffusion to occur (Welch and Easterby, 1994). GFP-fusion constructs with proteins of different sizes would permit studies of the dependence of solute diffusion on solute size, or "solute sieving" (Luby-Phelps et al., 1986). In addition, cells strongly expressing GFP should be suitable for studies of GFP translational diffusion in membrane-adjacent cytoplasm by total internal reflection photobleaching (Swaminathan et al., 1996), as well as measurements of slow GFP-membrane protein rotation by polarized photobleaching recovery (Velez and Axelrod, 1988).

For use in photobleaching recovery, GFP should be brightly fluorescent when excited by a continuous-wave ion laser and be bleached irreversibly with good efficiency. In addition, reversible photobleaching involving triplet-state relaxation or other processes should be minimal, easily distinguished from irreversible photobleaching, or eliminated by maneuvers such as solution oxygenation (as was done for fluorescein; Swaminathan et al., 1996). For analysis of GFP rotation by anisotropy decay and polarized photobleaching recovery, the intrinsic anisotropy of the GFP chromophore should be high and chromophore segmental motion should be minimal. An initial purpose of this study was to characterize the photochemical properties of GFP that are relevant for its use in photobleaching and polarization measurements. The GFP mutant S65T was

Received for publication 9 December 1996 and in final form 10 January 1997.

Address reprint requests to Dr. Alan S. Verkman, Cardiovascular Research Institute, 1246 Health Sciences East Tower, Box 0521, University of California, San Francisco, San Francisco, CA 94143-0521. Tel.: 415-476-8530; Fax: 415-665-3847; E-mail: verkman@itsa.ucsf.edu.

0006-3495/97/04/1900/08 $2.00

chosen because of its bright green fluorescence when excited with the 488-nm line of an argon laser (Heim et al., 1995; Heim and Tsien, 1996). Studies using recombinant purified GFP in solution and GFP transfected in cell cytoplasm indicated that GFP-S65T has suitable photochemical properties for cellular photobleaching and polarization measurements. Spot photobleaching was then used to quantify GFP translational diffusion in cell cytoplasm, and time-resolved anisotropy was used to quantify GFP rotational diffusion. The studies provide the first information about the translational and rotational diffusion of a macromolecule-size solute in the cytoplasm of a noninjected cell.

MATERIALS AND METHODS

Chemicals

Fluorescein was purchased from Molecular Probes. α-(4-Pyridyl-1-oxide)-*N*-*t*-butylnitrone (4-POBN), 2-mercaptoethylamine (MEA), 1,4-diazabicyclo-[2.2.2.] octane (DABCO), dextrans, D-tryptophan, L-histidine, and other chemicals were purchased from Sigma.

GFP protein expression and purification

GFP-S65T was constructed by oligonucleotide-directed mutagenesis using the Altered Sites II Mutagenesis System (Promega). The GFP-S65T coding sequence was confirmed by sequence analysis and subcloned into *Bam*HI and *Hin*dIII restriction sites of expression plasmid pRSETB (Invitrogen), which encodes a fusion protein containing a six-amino acid histidine tag and an enterokinase cleavage site upstream from the GFP-S65T insert. For bacterial expression, *Escherichia coli* BL21(DE3) pLysS (Novagen) was transformed with the expression plasmid and grown on LB plates containing 100 μg/ml ampicillin. A 300-ml overnight culture was used to inoculate 2700 ml of medium. The bacteria were grown at 30°C to an optical density of 0.6–0.8 at 600 nm (~1.5 h) and induced with 1 mM IPTG for 3–4 h. Cells were recovered by centrifugation and lysed by sonication after the addition of 1 mg/ml lysozyme in 50 ml phosphate buffer (50 mM Na phosphate, 300 mM NaCl, pH 8.0) at 4°C for 30 min. After sonication, DNase I (5 μg/ml) and ribonuclease A (10 μg/ml) were added. After centrifugation, the supernatant containing soluble GFP-S65T was purified by metal chelation chromatography using a Ni^{2+}-nitrilotriacetic acid (Ni-NTA) affinity resin. Buffer composition and elution procedures were as specified by the manufacturer. The eluted protein was judged to be >98% pure by Commassie blue-stained sodium dodecyl sulfate-polyacrylamide gel electrophoresis. GFP-S65T was stored as a dessicated solid after dialysis against 5 mM sodium phosphate (pH 7.4) and lyophilization. Protein yield was 10–20 mg/liter of bacterial culture.

GFP transfection and cell culture

Cell transfection and selection of clonal cell populations were carried out as described (Yang et al., 1996). The GFP-S65T coding sequence from plasmid pRSET (above) was subcloned into vector pcDNA3 (Invitrogen) and propagated in *E. coli*. CHO-K1 (wild-type) cells were grown in Ham's Nutrient Mix supplemented with 10% fetal calf serum at 37°C in 5% CO_2/95% air. Cells were plated at a density of 5×10^5 per 60-mm-diameter dish 12 h before transfection. Cells were washed with Opti-MEM1 media (GIBCO, BRL) and then incubated for 12 h at 37°C with 2 ml of medium containing 20 μg Lipofectin (GIBCO, BRL) and 10 μg of plasmid pcDNA3 containing the GFP-S65T insert. Cells were washed and incubated for 24 h in 4 ml of Ham's Nutrient Mix containing 10% fetal calf serum. Cells were trypsinized and plated on 100-mm-diameter dishes, and Geneticin (G418, GIBCO, BRL) was added (500 μg/ml) for selection. At 10–14 days, G418-resistant cell clones were isolated and transferred to separate culture dishes for expansion and selection by fluorescence microscopy. For experiments, cells were grown on fused silica coverslips until just confluent.

Fluorescence recovery after photobleaching

Spot photobleaching recovery measurements were carried out on an apparatus described previously (Kao and Verkman, 1996). The output of an Argon ion laser (488 nm, Innova 70-4; Coherent, Inc.) was modulated by serial acoustooptic modulators and reflected onto the stage of an inverted epifluorescence microscope (Diaphot, Nikon) by a 510-nm dichroic mirror. Unless otherwise specified, a 20× dry objective lens (Nikon, numerical aperture 0.75) was used. Sample fluorescence was filtered by serial interference (530 ± 15 nm) and cut-on (>515 nm) filters and detected by a gated photomultiplier. The minimum instrument bleach time was 1 μs, and the maximum rate of data acquisition (14-bit) was 1 MHz. Probe beam intensity and probe-to-bleach beam attenuation ratio (generally 2000–8000:1) were specified to avoid photobleaching during the probe period. Software was used to record prebleach and postbleach signals, to modulate laser beam intensity, and to reduce photomultiplier gain during photobleaching. Signals were sampled before the bleach (generally 10^3 data points in 100 ms) and over three different time intervals after the bleach: high-resolution data (1 MHz sampling rate) over 10–100 ms, low-resolution data (generally 10^4 points) over 0.1–10 s, and "final signal" data (10^3 points) at late times after nearly complete recovery has occurred. High- and low-resolution data were binned into 200 points each for storage and analysis.

For measurements in aqueous solutions, 5-μl solution volumes were "sandwiched" between two fused silica coverslips. For cell measurements, the upper coverslip contained the cultured cells (facing downward). The sample was enclosed in a Lucite chamber in which the atmosphere could be controlled (humidified air, 100% nitrogen or oxygen). Generally, data from 5–20 individual recovery curves were averaged; in cell studies, each recovery curve was obtained from a different spot. All measurements were performed at room temperature.

Time-resolved fluorescence

Fluorescence lifetime and anisotropy decay measurements were carried out in the frequency domain by cuvette fluorimetry using a Fourier transform fluorimeter (48000 MHF; SLM Instruments, Urbana, IL), or by fluorescence microscopy using epifluorescence microscope optics in place of the cuvette compartment (Fushimi and Verkman, 1991). For microscopy measurements, the impulse-modulated, vertically polarized light (488 nm) was reflected onto the sample by a 510-nm dichroic mirror and objective lens; emitted fluorescence was filtered by a 515-nm cut-on filter and passed through a rotatable analyzing calcite polarizer. In some experiments, a biconcave lens was introduced just in front of the dichroic mirror to broaden the beam diameter to ~40 μm.

Analysis of lifetime and time-resolved anisotropy was performed by a comparative approach. Generally four pairs of measurements (each acquisition 6.9 s) were obtained, comparing sample and reference (fluorescein in 0.1 N NaOH, lifetime 4.0 ns) for measurement of lifetime, and parallel and perpendicular orientations of the emission polarizer for measurement of anisotropy decay. The phase-modulation data consisted of phase angles and modulation ratios at 40 discrete, equally spaced modulation frequencies (5–200 MHz). The analyzing polarizer was positioned at the magic angle for lifetime measurements. Other details of the data acquisition and analysis routines were described previously (Verkman et al., 1991). Anisotropy decay measurements required the inclusion of a geometric factor (generally ~1.2) to correct for the differential detection of parallel versus perpendicular emission polarization arising mainly from differential reflectivity of the dichroic mirror (Verkman et al., 1991). The geometric factor was determined using a dilute solution of fluorescein in 0.1 N NaOH (rotational correlation time 120 ps). Modulation ratio values at each frequency were divided by the geometric factor. Median phase and modulation values for

paired data were analyzed by nonlinear least-squares for determination of lifetimes and rotational correlation times.

RESULTS

Fluorescence properties of purified GFP

GFP-S65T was expressed in bacteria and purified as described in Materials and Methods. Fluorescence spectra in PBS (pH 7.4) showed single excitation and emission maxima at 492 and 509 nm (Fig. 1 *A*), respectively, in agreement with previous results (Heim et al., 1995). The GFP-S65T molar absorbance at the excitation maximum was 41,800 M^{-1} cm^{-1}, and the quantum yield was 0.70. Measurement of fluorescence intensity decay by phase-modulation fluorimetry showed a single lifetime in PBS of 2.93 ± 0.02 ns (SE, n = 7) (Fig. 1 *B*), which was independent of pH in the range 5–11.

A plot of differential phase and modulation amplitude ratio for GFP-S65T in PBS is shown in Fig. 1 *C*. Generally, the data fitted best to a two-rotator anisotropy decay model, with a major component (fractional amplitude 0.86–0.91) of 20 ± 1 ns (n = 8) and a variable minor component of (0.01–1 ns). The predicted steady-state anisotropy for the data shown in Fig. 1 *C* was 0.320, which agreed well with the measured anisotropy of 0.325. It was concluded that the major component represented rotation of the whole GFP protein and that the variable minor component was an artifact related to light scattering or instrument noise. This interpretation was supported by measurements of GFP anisotropy decay in solutions of increasing viscosity (see Fig. 5, below) and estimates of rotational correlation time based on GFP size (see Discussion).

Photobleaching properties of purified GFP

Fig. 2 shows an analysis of irreversible photobleaching of GFP-S65T in PBS by spot photobleaching. In response to a brief bleach pulse, GFP fluorescence promptly decreased and then recovered to its initial level in a monophasic manner (Fig. 2 *A*). For comparison, photobleaching of fluorescein in PBS is shown; under the same bleach conditions, the recovery half-time ($t_{1/2}$) for fluorescein was threefold faster than that for GFP, and the depth of photobleaching for

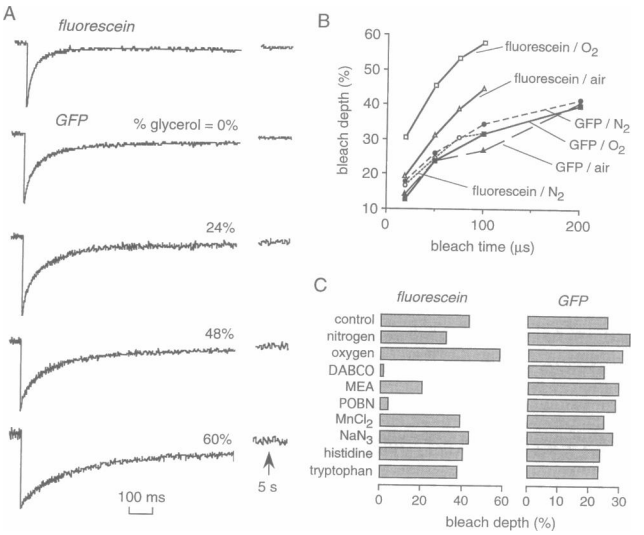

FIGURE 2 Irreversible photobleaching of GFP-S65T. (*A*) Spot photobleaching of fluorescein (58 μM) in 0.1 N NaOH or GFP-S65T (30 μM) in PBS using 100-μs bleach time and 5-μm spot diameter (20× objective). Indicated percentages of glycerol were added to the PBS in GFP-S65T studies. (*B*) Bleach depth versus bleach time for spot photobleaching of fluorescein and GFP-S65T. Bleach depth was expressed as the percentage of fluorescence signal just after versus before the bleach pulse. Data are shown for solutions equilibrated with air, 100% O_2, or 100% N_2. (*C*) Summary of bleach efficiencies for a series of maneuvers. Bleach efficiency was defined as bleach depth at 100 μs bleach time. Solutions consisted of fluorescein or GFP-S65T in PBS equilibrated with O_2 or N_2 as in *B*, or PBS containing DABCO (100 mM), MEA (100 mM), 4-POBN (100 mM), $MnCl_2$ (25 mM), NaN_3 (5 mM), histidine (5 mM), or *d*-tryptophan (25 mM).

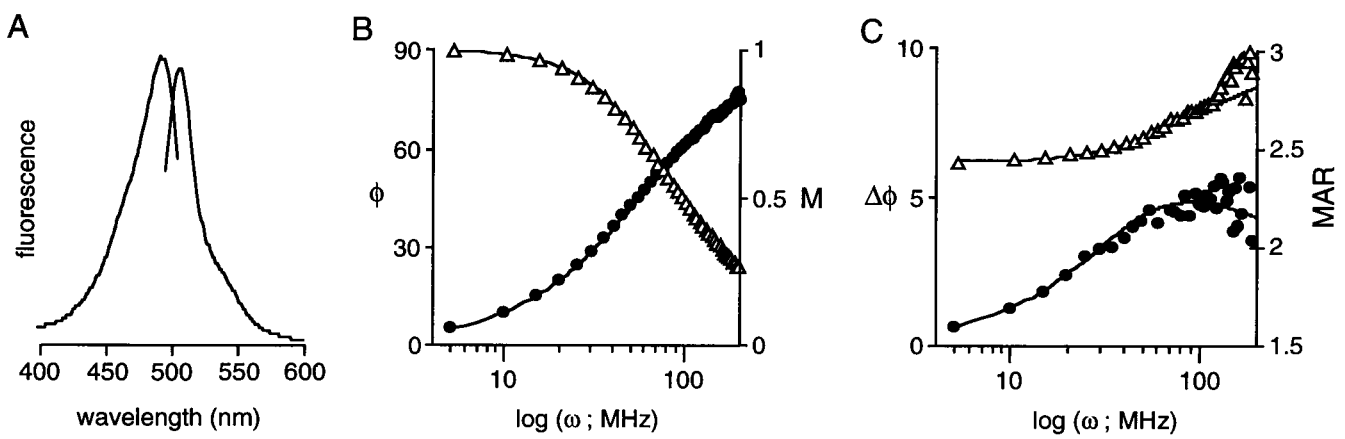

FIGURE 1 Fluorescence spectra and time-resolved fluorescence properties of GFP-S65T (16 μM) in PBS. (*A*) Excitation spectrum at 509-nm emission wavelength and emission spectrum at 492-nm excitation wavelength. (*B*) Phase-modulation plot of fluorescence lifetime decay showing phase angles (ϕ, ●) and modulation amplitudes (M, △) as a function of modulation frequency (ω). Fitted curves correspond to a lifetime of 2.9 ns. (*C*) Anisotropy decay plot of differential phase angle ($\Delta\phi$, ●) and modulation amplitude ratio (MAR, △). Fitted curves corresponding to a two-component anisotropic decay model with rotational correlation times of 19 ns (fractional amplitude, 0.91) and 0.74 ns.

fluorescein was about twofold greater. The deduced GFP-S65T diffusion coefficient from the $t_{1/2}$ value was 8.67 × 10^{-7} cm^2/s, in agreement with that of 8.7 × 10^{-7} cm^2/s for wild-type GFP determined by fluorescence correlation microscopy (Terry et al., 1995). The $t_{1/2}$ for the recovery process was linearly related to solution viscosity (Fig. 2 *A*, and see Fig. 4 *B*, below), strongly dependent on laser spot size, and independent of GFP concentration (range 10–70 μM) (see below). The recovery process was thus attributed to GFP translational diffusion after irreversible photobleaching. Interestingly, solution oxygen content did not affect GFP photobleaching efficiency.

A series of possible modulators of GFP photobleaching were tested by measurement of the dependence of bleach depth on bleach time at constant laser beam intensity. Fig. 2 *B* shows bleach depth versus bleach time for PBS solutions equilibrated with air, oxygen, or nitrogen. The bleach efficiency for fluorescein, but not GFP-S65T, was increased with increasing solution oxygen content. Fig. 2 *C* summarizes the relative bleach efficiencies for measurements performed in PBS solutions having different oxygen contents and various additives. Whereas photobleaching of fluorescein was strongly influenced by some general radical quenchers (MEA and 4-POBN) and singlet oxygen scavengers (DABCO), in agreement with previous results (Song et al., 1996), photobleaching of GFP-S65T was insensitive to solution oxygen content and each of the compounds tested. This was an unexpected finding that may relate to the inaccessibility of the GFP chromophore to compounds present in the external solution (see Discussion).

The photobleaching measurements of GFP-S65T in PBS above showed no evidence for reversible (not dependent on GFP-S65T translational diffusion) photobleaching. To search for possible reversible photobleaching processes that might be observable in the relatively viscous cellular environment, photobleaching of the purified GFP-S65T protein was done in air-equilibrated aqueous solutions of PBS made viscous with various concentrations of glycerol. Fig. 3 *A* shows the appearance of a rapid recovery process with $t_{1/2}$ of 3.1, 4.0, and 5.5 ms in solutions of relative viscosity 10 (60% glycerol), 60 (80% glycerol), and 250 (90% glycerol). (This fast process was not observed in Fig. 2 *A* because of the longer bleach time and lower glycerol concentration.) The $t_{1/2}$ values of 3.1–5.5 ms are too small to arise from GFP translational diffusion, and thus the fast recovery process was presumed to arise from reversible photobleaching. To support this interpretation, photobleaching measurements were carried out by using different laser spot diameters (by use of 10× versus 20× objective lenses). Fig. 3 *B* shows that whereas the recovery from irreversible photobleaching was strongly dependent on spot diameter, the reversible process was not (from three sets of measurements: $t_{1/2}$ = 1.43 and 230–400 ms [10×]; $t_{1/2}$ = 1.57 and 120 ms, [20×]). Further studies were carried out to investigate the mechanism of the putative reversible photobleaching process. Fig. 3 *C* shows the dependence of the GFP-S65T fluorescence recovery on bleach time. The relative

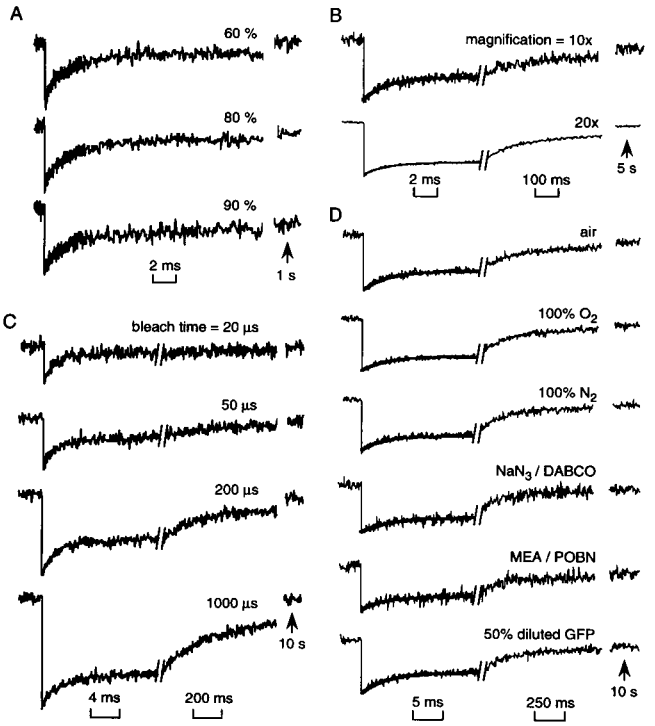

FIGURE 3 Reversible photobleaching of GFP-S65T. (*A*) Solutions consisted of 30 μM GFP-S65T in PBS containing indicated glycerol concentrations. Spot bleaching was done with 20× objective and 30 μs bleach time. (*B*) Effect of spot diameter. Experiments were done for GFP-S65T in PBS containing 48% glycerol with 100 μs bleach time, using 10× and 20× objectives. (*C*) Effect of bleach time. Experiments were done as in *B*, using 60% glycerol and 20× objective and indicated bleach times. (*D*) Effect of possible modulators of reversible photobleaching. Experiments were done with GFP-S65T (66 μM) in PBS equilibrated with O_2 or N_2, and PBS containing indicated additives (see legend to Fig. 2 for concentrations). Bleach time was 100 μs and glycerol concentration was 60%. Where indicated (50% diluted GFP), the GFP-S65T concentration was diluted twofold (in air-equilibrated PBS). Fitted $t_{1/2}$ values for the reversible photobleaching (fit shown) were in the range 3.05–3.34 ms.

amplitude of the irreversible-to-reversible recovery processes increased with increasing bleach time, suggesting the involvement of triplet-state relaxation (Periasamy et al., 1996). Triplet-state relaxation was proved for fluorescein from the dependence of $t_{1/2}$ for the rapid recovery process on solution oxygen content and triplet state quenchers. Fig. 3 *D* shows that under conditions where the reversible photobleaching of fluorescein was strongly affected, there was no effect on GFP-S65T recovery. GFP-S65T concentration also did not affect recovery (Fig. 3 *D*, *bottom curve*), making a dimerization mechanism (Stout and Axelrod, 1995) unlikely. These results indicate that GFP-S65T can undergo reversible photobleaching in air-equilibrated solutions only a few times more viscous than water.

Translational diffusion of GFP in cytoplasm

Spot photobleaching measurements were made in stably transfected cells expressing GFP in the cytoplasm. Fig. 4 *A*

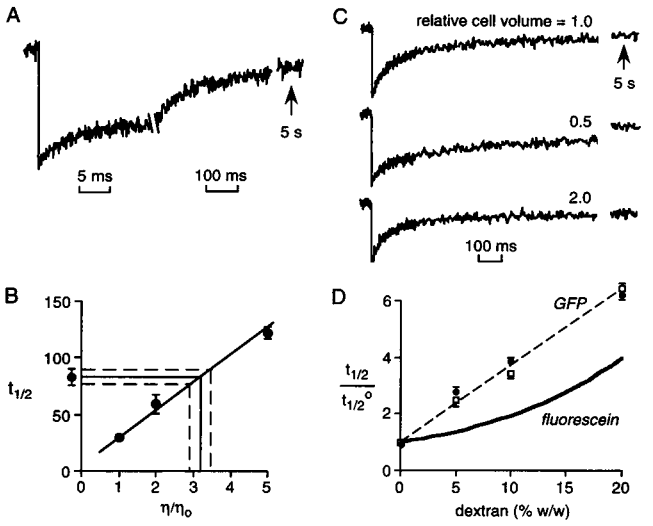

FIGURE 4 Translational diffusion of GFP-S65T in cytoplasm. (*A*) Spot photobleaching (20× objective) was carried out in cells expressing GFP-S65T using 50 μs bleach time. Note the presence of a fast recovery process from reversible photobleaching and slower recovery resulting from GFP diffusion (see text). (*B*) Determination of relative cytoplasmic viscosity. Recovery half-times ($t_{1/2}$) in ms for GFP-S65T diffusion in PBS containing glycerol (see Fig. 2 *A*) plotted against relative solution viscosity. Data for GFP-S65T diffusion in cytoplasm are indicated. (*C*) Recovery curves as in *A*, for cells in PBS (relative volume, 1.0) and after brief incubation with PBS containing 300 mM sucrose (relative volume, 0.5) or 1:1 PBS:water (relative volume 2.0). (*D*) Influence of solution crowding on GFP-S65T diffusion. Solutions consisted of GFP-S65T in PBS containing indicated concentrations of dextran (19 kDa, □; 70 kDa, ●). The ordinate is $t_{1/2}$ for photobleaching recovery with versus without ($t_{1/2}^o$) dextran. The curve for diffusion of fluorescein was taken from Kao et al. (1993) and confirmed here.

shows representative recovery data. As in aqueous solutions containing glycerol, well-separated reversible and irreversible recovery processes were observed. The rate of the rapid, reversible recovery process was independent of laser spot diameter, whereas that of the irreversible process was strongly dependent (data not shown). An irreversible recovery process was observed that was 82 ± 2% complete (n = 6), indicating that the majority of cytoplasmic GFP-S65T was mobile. To determine the relative viscosity of cytoplasm compared to water (same viscosity as PBS), $t_{1/2}$ for the irreversible recovery process (83 ± 6 ms) in cytoplasm was compared to $t_{1/2}$ measured for diffusion of purified GFP-S65T in solutions of known viscosity (Fig. 4 *B*). The interpolated relative viscosity of cytoplasm (versus water) was 3.2 ± 0.3.

In a previous study (Kao et al., 1993), the cytoplasmic diffusion coefficient of the small solute BCECF was dependent upon cell volume, increasing significantly with increasing cell volume. Similar studies were carried out for the GFP-expressing cells exposed to osmotic gradients to induce cell swelling and shrinkage. Fig. 4 *C* shows accelerated recovery (1.6-fold) in swollen cells and slowed recovery (2.9-fold) in shrunken cells. To investigate whether obstacles in the cytoplasm could account for this observation, measurements were made of GFP-S65T diffusion in PBS solutions containing dextran. Fig. 4 *D* shows an increase in $t_{1/2}$ with dextran concentration; similar results were obtained for 19-kDa and 70-kDa dextrans. The apparent relative viscosity of cytoplasm computed from Fig. 4 *B*, 3.2 ± 0.3, is seen in Fig. 4 *D* to be equivalent to a dextran concentration of ~8 wt%. A twofold decrease in dextran concentration to 4 wt% (expected cytoplasmic dilution for twofold cell swelling) resulted in a 1.6-fold decrease in $t_{1/2}/t_{1/2}^o$, in exact agreement with the 1.6-fold accelerated recovery in swollen cells. A twofold increase in dextran concentration to 16 wt% resulted in a 1.7-fold increase in $t_{1/2}/t_{1/2}^o$, somewhat less than the 2.9-fold slowed recovery in the shrunken cells. These results are in agreement with our previous conclusion that solute translational mobility in cytoplasm is determined primarily by the concentration of obstacles. For comparison, Fig. 4 *D* shows the results from Kao et al. (1993) for diffusion of fluorescein in dextran solutions. We note that as predicted by Furukawa et al. (1991), GFP "senses" a higher apparent solution viscosity than that sensed by the small fluorescein molecule.

Rotational diffusion of GFP in cytoplasm

If cytoplasm acts as a nonviscous crowded solution of macromolecules with respect to solute diffusion, then cytoplasm should hinder solute rotation to a lesser extent than solute translation. This was the case for BCECF rotation in cytoplasm, which was only 1.1–1.4-fold slower than that in water (Fushimi and Verkman, 1991; Bicknese et al., 1993), compared to 3.7-fold slowed BCECF translation (Kao et al., 1993). Rotation of GFP-S65T in cytoplasm was measured by time-resolved anisotropy using fluorescence microscopy. Fig. 5 *A* shows a single fluorescence lifetime of 2.6 ± 0.1 ns (n = 3) for GFP-S65T in cytoplasm, similar to that for GFP-S65T in PBS. Fig. 5 *B* shows a phase-modulation plot of anisotropy decay, which gave a best-fit rotational correlation time of 36 ± 2 ns (n = 5). To determine the apparent cytoplasmic viscosity as sensed by GFP-S65T rotation, the rotational correlation time in cytoplasm was compared to that measured in solutions of known viscosity (Fig. 5 *C*). The relative viscosity was 1.5 ± 0.1.

To determine whether this minor slowing of GFP rotation is consistent with the view that cell cytoplasm acts like a crowded solution of macromolecules, the influence of dextran on GFP-S65T rotation was measured. Previous studies showed that rotation of a small solute (<0.5 kDa, e.g., fluorescein) in water is unaffected by the addition of relatively large dextrans (Fushimi and Verkman, 1991). Similar measurements were carried out using purified GFP-S65T in aqueous saline solutions containing different dextran concentrations, and using dextrans of two sizes, one smaller (19 kDa) and the other larger (70 kDa) than GFP. Fig. 5 *D* shows that GFP-S65T rotation was slowed progressively as the solution became more crowded with increasing dextran concentration. The GFP-S65T rotational correlation time

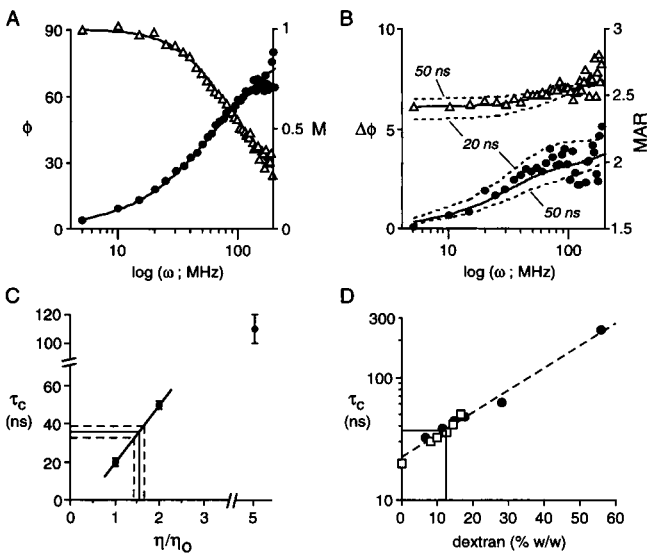

FIGURE 5 Rotational diffusion of GFP-S65T in cytoplasm. (*A*) Phase-modulation plot of GFP-S65T lifetime in cytoplasm. The fitted lifetime was 2.6 ns. (*B*) Differential phase-modulation plot of GFP-S65T anisotropy decay with correlation times of 34 ns (fractional amplitude, 0.85) and 0.3 ns. Dashed curves indicate where the data would fall for correlation times of 20 and 50 ns instead of 34 ns. (*C*) Determination of relative cytoplasmic viscosity. Rotational correlation times for GFP-S65T in PBS containing glycerol plotted against relative solution viscosity. Data for GFP-S65T rotation in cytoplasm are indicated. (*D*) Dependence of GFP-S65T rotational correlation time on dextran concentration for 19 kDa (□) and 70 kDa (●) dextrans.

measured in cell cytoplasm above, 36 ns, was obtained in the solution containing ~12 wt% for both the 19-kDa and 70-kDa dextrans. These values are in the general range of macromolecule concentrations found in cytoplasm (8–20 wt%) (see Discussion).

DISCUSSION

The purposes of this study were to evaluate the suitability of GFP as a probe for rapid solute diffusion in living cells and to measure the apparent viscosity of cell cytoplasm from the rates of GFP translational and rotational diffusion. The GFP mutant S65T with red-shifted excitation spectrum was expressed in bacteria, purified, and shown to be highly fluorescent when excited at the argon laser wavelength of 488 nm. In nonviscous saline, GFP-S65T underwent irreversible photobleaching with an efficiency about twofold lower than that for fluorescein. The relative photostability of GFP-S65T is advantageous because greater probe beam intensities can be used with minimal photobleaching during the probe period. GFP-S65T did not yield a detectable signal from reversible photobleaching when in nonviscous solutions; however, as found for fluorescein (Periasamy et al., 1996; Swaminathan et al., 1996), reversible photobleaching probably involving triplet-state relaxation was detected in air-equilibrated viscous solutions and in cells. Time-resolved anisotropy measurements indicated that the GFP-S65T chromophore was rigidly coupled to total protein rotation. These photochemical properties were exploited to quantify the rates of GFP-S65T translation and rotation in the cytoplasm of living cells.

For irreversible photobleaching of GFP-S65T, the $t_{1/2}$ for fluorescence recovery was linearly related to solution viscosity and was strongly dependent on laser spot size. Similar results were obtained for irreversible photobleaching of fluorescein (Kao et al., 1993). However, unlike fluorescein, where the photobleaching efficiency was affected by several general radical quenchers and singlet oxygen scavengers, photobleaching of GFP-S65T was insensitive to these maneuvers. This insensitivity may be related to the inaccessibility of dissolved solutes to the GFP chromophore. The recent GFP crystal structure (Ormo et al., 1996) indicates that the chromophore is completely shielded from bulk solvent by a dense, 11-stranded β-barrel.

In addition to the irreversible recovery process, a more rapid reversible recovery process was found for photobleaching of GFP-S65T in air-saturated viscous solutions. The $t_{1/2}$ for recovery from reversible photobleaching was in the millisecond range and did not depend upon laser spot size, indicating that it did not involve GFP-S65T translational diffusion. In addition, as found for reversible photobleaching of fluorescein (Periasamy et al., 1996), the reversible recovery of GFP-S65T was slowed in a nonlinear manner in solutions of increasing viscosity, and the relative amplitudes of reversible-to-irreversible photobleaching recovery were dependent on laser bleach time and intensity. These findings suggest that the reversible recovery of GFP-S65T involves triplet state relaxation; however, unlike fluorescein, reversible recovery of GFP-S65T was insensitive to solution O_2 content and triplet-state quenchers. As discussed above, the inaccessibility of the GFP chromophore may be responsible for its insensitivity to triplet-state quenchers, although other mechanisms of reversible photobleaching cannot be ruled out. Confirmation of triplet-state involvement will require measurement of phosphorescence spectra and direct determination of the triplet state lifetime. Mechanisms involving monomer-monomer interactions, as proposed for reversible recovery of surface-adsorbed fluorophores (Stout and Axelrod, 1995), probably do not operate here, based on the observation that GFP-S65T reversible photobleaching did not depend on GFP-S65T protein concentration.

Time-resolved fluorescence measurements of GFP-S65T in aqueous solutions indicated a single lifetime of 2.9 ns, which was similar to that measured in cell cytoplasm. Time-resolved anisotropy of GFP-S65T in nonviscous saline solution revealed slow rotation with a correlation time of 20 ns. This slow correlation time indicates that the chromophore is held rigidly within the GFP molecule, a conclusion supported by the crystal structure of GFP. It was remarkable that chromophore segmental motions with short rotational correlation times were absent, a finding very different from that in exogenously labeled proteins (Thevenin et al., 1994), where the depolarization is dominated by

segmental motions. The Stokes-Einstein relation predicts a rotational correlation time of 13 ns for a 31.1-kDa spherical protein (size of GFP-S65T with N-terminus polyhistidine tag and enterokinase cleavage site), somewhat less than that observed here. However, because the fluorescence lifetime of GFP-S65T was considerably less than its rotational correlation time, it was not possible to resolve anisotropic rotations related to nonspherical shape or GFP dimerization. A previous study indicated that significant dimerization of wild-type GFP did not occur at concentrations under 74 μM (Chalfie, 1995). The nonspherical GFP shape based on crystal structure (approximate cylinder of 2.4 nm diameter, 4.2 nm height; Ormo et al., 1996) predicts anisotropic rotation with correlation times of 20.4 and 13.6 ns (after correction for hydration), based on the rotations of a prolate ellipsoid (Cantor and Schimmel, 1980). The 20-ns apparent correlation time measured here thus probably represents an average of several correlation times.

In cell cytoplasm, the GFP rotational correlation time was 36 ns, 1.5-fold slower than that in nonviscous saline solution. There was no evidence for GFP binding to intracellular structures, which would slow apparent GFP rotation. The rapid GFP rotational rate in cytoplasm is consistent with the notion that particle rotation is relatively unhindered when particle size is smaller than the spacings between obstacles (Drake and Klafter, 1990). It was found previously that rotation of the fluorescein-like probe BCECF was 1.1–1.4 times slower in cytoplasm than in water (Fushimi and Verkman, 1991). The slightly slowed rotation of GFP-S65T (relative to water) compared to that of BCECF may be related to steric interactions with intracellular macromolecules. This possibility was supported by the slowed GFP-S65T rotation in solutions containing dextrans. Further definition of the constraints to macromolecule rotation in cells will require measurements of the rotation of GFP-fusion adducts of greater size and defined shape.

The kinetics of GFP fluorescence recovery in transfected cells provide the first data on the translational mobility of a macromolecule in a nontraumatized cell. Previous studies of macromolecule diffusion in cytosol have utilized single-cell microinjection of fluorescently labeled dextrans (Luby-Phelps et al., 1986), Ficolls (Luby-Phelps et al., 1987), or proteins such as calmodulin (Luby-Phelps et al., 1995). It has been difficult to address concerns about traumatic effects of the microinjection procedure, including cytoskeletal disruption and defective cell volume regulation. Comparison of $t_{1/2}$ values for GFP diffusion in cytosol and water indicated that GFP translational diffusion in cytosol is reduced by ~3.2-fold compared to that in water. In prior studies of the diffusion of FITC-dextran and FITC-Ficoll in cytoplasm of Swiss 3T3 fibroblasts (Luby-Phelps et al., 1986, 1987), macromolecules of ~30 kDa (~3.2-nm radius) were slowed ~5-fold (dextran) and 3.5-fold (ficoll) in cytosol versus water. In a preliminary study of FITC-dextran diffusion in the cytosol of MDCK cells and Swiss 3T3 fibroblasts (Seksek and Verkman, 1997), 2.6–3.8-fold slowing was observed for FITC-dextran of 4–2000 kDa. The 3.2-fold slowing of GFP translation in cytoplasm was thus similar to that found for dextrans of comparable size. As discussed in reference to Fig. 4 *D*, the further slowing of GFP translation in shrunken cells and the acceleration of GFP translation in swollen cells is consistent with the barrier properties of intracellular obstacles. Further analysis of proposed solute sieving mechanisms (Luby-Phelps et al., 1986, 1987) will require photobleaching measurements on larger GFP-fusion adducts.

In summary, the data here indicate that GFP-S65T is suitable for photobleaching recovery and time-resolved anisotropy measurements of solute mobility in the cellular environment, with the caveat that reversible photobleaching processes must be identified and, if necessary, taken into account. In addition to studies of aqueous-phase solute diffusion in cytoplasm, mitochondria, and other fluid compartments as mentioned in the Introduction, the lateral mobility of GFP-tagged membrane proteins in the plane of the membrane should be measurable by photobleaching methods. The high intrinsic anisotropy of GFP-S65T and the lack of depolarizing segmental dynamics should permit measurements of the rotation of GFP-labeled membrane proteins by polarized photobleaching methods. Finally, the cell data here constitute the first measurement of macromolecule rotational mobility in cytoplasm, as well as the first noninvasive measurement of macromolecule translational mobility in a nontraumatized cell.

We thank Katherine Chen for cell culture, Dr. C. Rozanas for help in GFP protein expression and purification, and Dr. N. Periasamy for helpful advice on photobleaching mechanisms.

This work was supported by grants DK43840, DK16095, and HL42368 from the National Institutes of Health. C.H. was supported by a summer student fellowship from the American Heart Association, California Affiliate.

REFERENCES

Bicknese, S., N. Periasamy, S. B. Shohet and A. S. Verkman. 1993. Cytoplasmic viscosity near the cell plasma membrane: measurement by evanescent field frequency-domain microfluorimetry. *Biophys. J.* 65: 1272–1282.

Cantor, C. R., and P. R. Schimmel. 1980. Biophysical Chemistry. Part II. Techniques for the Study of Biological Structure and Function. W. H. Freeman and Co., New York. 562–565.

Chalfie, M. 1995. Green fluorescent protein. *Photochem. Photobiol.* 62: 651–656.

Chalfie, M., Y. Tu, G. Euskirchen, W. W. Ward, and D. C. Prasher. 1994. Green fluorescent protein as a marker for gene expression. *Science.* 263:802–805.

Cole, N. B., C. L. Smith, N. Sciaky, M. Terasaki, M. Eddin, and J. Lippincott-Schwartz. 1996. Diffusional mobility of Golgi proteins in membranes of living cells. *Science.* 273:797–801.

Cubitt, A. B., R. Heim, S. R. Adams, A. E. Boyd, L. A. Gross, and R. Y. Tsien. 1995. Understanding, improving and using green fluorescent proteins. *Trends Biochem. Sci.* 20:448–455.

Drake, R. D., and J. Klafter. 1990. Dynamics of confined molecular systems. *Phys. Today.* 43:46–55.

Furukawa, R., J. L. Arauz-Lara, and B. R. Ware. 1991. Self-diffusion and probe diffusion in dilute and semidilute aqueous solutions of dextran. *Macromolecules.* 24:599–605.

Fushimi, K., and A. S. Verkman. 1991. Low viscosity in the aqueous domain of cytoplasm measured by picosecond polarization microscopy. *J. Cell Biol.* 112:719–725.

Gerdes, H.-H., and C. Kaether. 1996. Green fluorescent protein: applications to cell biology. *FEBS Lett.* 389:44–47.

Giorgi, F. D., M. Brini, C. Bastianutto, R. Marsault, M. Montero, P. Pizzo, R. Rossi, and R. Rizzuto. 1996. Targetting aequorin and green fluorescent protein to intracellular organelles. *Gene.* 173:113–117.

Heim, R., A. B. Cubitt, and R. Y. Tsien. 1995. Improved green fluorescence. *Nature.* 373:663–664.

Heim, R., and R. Y. Tsien. 1996. Engineering green fluorescent protein for improved brightness, longer wavelengths and fluorescence resonance energy transfer. *Curr. Biol.* 6:178–182.

Kao, H. P., J. R. Abney, and A. S. Verkman. 1993. Determinants of the translational diffusion of a small solute in cytoplasm. *J. Cell Biol.* 120:175–184.

Kao, H. P., and A. S. Verkman. 1996. Construction and performance of a FRAP instrument with microsecond time resolution. *Biophys. Chem.* 59:203–210.

Luby-Phelps, K. 1994. Physical properties of cytoplasm. *Curr. Opin. Cell Biol.* 6:3–9.

Luby-Phelps, K., P. E. Castle, D. L. Taylor, and F. Lanni. 1987. Hindered diffusion of inert tracer particles in the cytoplasm of mouse 3T3 cells. *Proc. Natl. Acad. Sci. USA.* 84:4910–4913.

Luby-Phelps, K., M. Hori, J. M. Phelps, and D. Won. 1995. Ca-regulated dynamic compartmentalization of calmodulin in living smooth muscle cells. *J. Biol. Chem.* 270:21521–21538.

Luby-Phelps, K., D. L. Taylor, and F. Lanni. 1986. Probing the structure of cytoplasm. *J. Cell Biol.* 102:2015–2022.

Ormo, M., A. B. Cubitt, K. Kallio, L. A. Gross, R. Y. Tsien, and S. J. Remington. 1996. Crystal structure of *Aequorea victoria* green fluorescent protein. *Science.* 273:1392–1395.

Periasamy, N., S. Bicknese, and A. S. Verkman. 1996. Reversible photobleaching of fluorescein conjugates in air-saturated viscous solutions: molecular tryptophan as a triplet state quencher. *Photochem. Photobiol.* 63:265–271.

Rizzuto, R., M. Brini, F. D. Giorgi, R. Rossi, R. Heim, R. Y. Tsien, and T. Pozzan. 1996. Double labelling of subcellular structures with organelle-targeted GFP mutants. *Curr. Biol.* 6:183–188.

Rizzuto, R., M. Brini, P. Pizzo, M. Murgia, and T. Pozzan. 1995. Chimeric green fluorescent protein: a new tool for visualizing subcellular organelles in living cells. *Curr. Biol.* 5:635–642.

Seksek, O., and A. S. Verkman. 1997. Translational diffusion of macromolecule-size solutes in cytoplasm and nucleus: evidence for diffusion-restricting compartments without sieving. *Biophys. J.* 72:A202. (Abstr.)

Song, L., C. A. G. O. Varma, J. W. Verhoeven, and H. J. Tanke. 1996. Influence of the triplet excited state on photobleaching kinetics of fluorescein in microscopy. *Biophys. J.* 70:2959–2968.

Stout, A. L., and D. Axelrod. 1995. Spontaneous recovery of fluorescence by photobleached surface-adsorbed proteins. *Photochem. Photobiol.* 62: 239–244.

Swaminathan, R., N. Periasamy, S. Bicknese, and A. S. Verkman. 1996. Cytoplasmic viscosity near the cell plasma membrane: translation of BCECF measured by total internal reflection-fluorescence photobleaching recovery. *Biophys. J.* 71:1140–1151.

Terry, B. R., E. K. Matthews, and J. Haseloff. 1995. Molecular characterisation of recombinant green fluorescent protein by fluorescence correlation microscopy. *Biochem. Biophys. Res. Commun.* 217:21–27.

Thevenin, B. J. M., N. Periasamy, S. B. Shohet, and A. S. Verkman. 1994. Segmental dynamics of the cytoplasmic domain of erythrocyte band 3 determined by time-resolved fluorescence anisotropy: sensitivity to pH and ligand binding. *Proc. Natl. Acad. Sci. USA.* 91:1741–1745.

Velez, M., and D. Axelrod. 1988. Polarized fluorescence photobleaching recovery for measuring rotational diffusion in solutions and membranes. *Biophys. J.* 53:575–591.

Verkman, A. S., M. Armijo, and K. Fushimi. 1991. Construction and evaluation of a frequency-domain epifluorescence microscope for lifetime and anisotropy decay measurements in subcellular domains. *Biophys. Chem.* 40:117–125.

Welch, R. G., and J. S. Easterby. 1994. Metabolic channeling versus free diffusion: translation-time analysis. *Trends Biochem. Sci.* 19:193–197.

Yang, B., D. Brown, and A. S. Verkman. 1996. The mercurial-insensitive water channel (AQP-4) forms orthogonal arrays in stably transfected CHO cells. *J. Biol. Chem.* 271:4577–4580.